9-2013

Correlational Study of Open Circuit Resonant (SansEC) Sensor's Electric Field Distribution on Lightning Attachment

Kayla M. Farrow
Old Dominion University, kfarr017@odu.edu

Linda L. Vahala
Old Dominion University, lvahala@odu.edu

CORRELATIONAL STUDY OF OPEN CIRCUIT RESONANT (SANSEC) SENSOR'S ELECTRIC FIELD DISTRIBUTION ON LIGHTNING ATTACHMENT

Kayla M. Farrow and Linda L. Vahala
Electrical and Computer Engineering Department
Old Dominion University
5115 Hampton Blvd Norfolk, VA 23529, USA
kfarr017@odu.edu

ABSTRACT

NASA Langley Research Center (LaRC) is conducting research to develop an open circuit SansEC (Sans Electric Connection) sensor to provide lightning strike protection (LSP) in conjunction with damage detection and diagnosis for composite aircraft. SansEC sensors are simplistic devices consisting of an open circuit conductive trace shaped in a planar geometric spiral. The length and width of the conductive trace as well as the gap separation between adjacent turns determines the inductance, resistance and capacitance of the LRC circuit and its associated resonant response. When the sensor is placed on a composite substrate, the electric impedance of the substrate is reflected in the sensors resonant response thus enabling it to detect permittivity and conductivity changes associated with composite damage. SansEC sensors can be designed in various shapes and sizes depending on the application. For applications on exterior aircraft surfaces, the sensor must be designed to perform the required lightning strike protection in addition to damage detection and diagnosis. [1] [2]

Lightning-direct effect current tests were conducted on multiple SansEC sensor configurations to evaluate their ability to withstand the incident lightning energy and protect the underlying composite. Test results indicated several SansEC sensor geometric configurations demonstrated an intrinsic ability to steer the lightning current along the corner of the sensor. To investigate this phenomenology, electromagnetic computational simulations were conducted to calculate the electric field distribution on the SansEC sensor's conductive trace to determine if the associated electromagnetic radiation preceding lightning attachment establishes modal structures on the conductive trace which predisposition the direction of the current flow. The simulations provide a means to visualize the trace's modal structure and identify electric field regions residing on the sensor. This paper presents a correlational study of the SansEC sensor's computed electric field distribution to the measured lightning propagation direction for various SansEC sensor configurations. The study suggests the direction of lightning propagation follows strong electric field regions resident on the conductive trace.

ACRONYMS AND SYMBOLS

A	:	Ampere
B	:	Magnetic Flux Density
C	:	Capacitance
E	:	Electric Field
ε_0	:	Free Space Permittivity
ε_r	:	Relative Permittivity
H	:	Magnetic Field
I	:	Current Amplitude
IR	:	Infra Red
l	:	length of sensor trace
L	:	Inductance
LSP:		Lightning Strike Protection
R	:	Resistance
$Tan\delta$:		Dielectric Loss Tangent
$\mu0$	:	Free Space Permeability
μr	:	Relative permeability
dB V/m:		Electric Field in Decibels
dB A/m:		Magnetic Field in Decibels

INTRODUCTION

A SansEC sensor is an open-circuit resonator composed of a single self-resonant coil made of conductive material usually in a planar spiral pattern or helix structure. The sensor is interrogated wirelessly in the magnetic near field. The sensor resonance is influenced by the electric impedance of materials within the boundary of its resonating near field. [1][2]

SansEC sensor technology is a new technical framework for designing, powering, and interrogating sensors to detect various types of damage in composite materials. The source cause of the in-service damage (lightning strike, impact damage, material fatigue, etc.) to an aircraft composite is secondary. The sensor will detect damage independent of the cause. Damage in composite material is generally associated with a localized change in material permittivity and/or conductivity. These changes are sensed using SansEC. The unique electrical signatures (amplitude, frequency, bandwidth, and phase) are used for damage detection and diagnosis. [1][2]

The NASA Aviation Safety Program Atmospheric Environmental Safety Technologies Project is conducting research to develop a multifunctional SansEC sensor technology to provide both lightning mitigation and damage detection and diagnosis for composite airframes. Lightning high current direct effect tests were conducted at the National Technical Systems' (NTS) Lightning Technologies (LTI) facility in Pittsfield, MA in February, 2012. Numerous SansEC geometry concepts were evaluated initially on fiberglass panels to develop an understanding of how the SansEC geometry influences lightning attachment and propagation on a dielectric substrate. [3]

The SansEC lightning test articles were housed in a lightning test bed during test current attachment to monitor the electrical current propagation off the four sides of the test panel to determine the propagation direction of the electric current. The test bed was also instrumented with an IR camera to measure the backside temperatures during the lightning strike. The SansEC conductive traces and ground paths generate resistive heating from the lightning current and temperature imagery allows visualization of lightning attachment and current propagation.

Several SansEC configurations demonstrated an intrinsic ability to propagate the lightning current along one corner of the sensor in effect steering the lightning currents. To investigate this phenomenon, computational simulations were developed to explore the characteristic electric and magnetic field structures on the SansEC sensor trace at its primary resonance frequency for these configurations. The frequency content of a lightning waveform falls within the operational frequency resonance bands for these SansEC configurations. As the lightning arc propagates toward the test panel its radiated electromagnetic field generates a self-resonance on the SansEC sensor establishing electric and magnetic field modal structures on the SansEC's spiral trace. Computational simulations were performed to visualize the electric and magnetic field structure residing on the SansEC trace and compared to the IR images to correlate high field strength with lightning attachment and propagation. This paper presents correlation for SansEC 7 inch, 8 inch and 9 inch square spiral configurations. [4]

MODEL GEOMETRIES

The first stage of this investigation was to generate accurate geometries of the lightning SansEC test panels. Figure 1 shows a picture of a lightning test panel with a 7 inch SansEC sensor and the ground path surrounding it before paint was applied. The end point of the SansEC spiral trace was always positioned in both experiment and simulation at the lower right corner with the trace proceeding in a clockwise manner to the center. The experimental panels were constructed of Fiberglass Reinforced Polymer (FRP) that was approximately 0.25 inch thick and 20x20 inches square. On top of the FRP was a 1.25 mil thick copper tape that encompassed the edges of the panel and the SansEC sensor. The SansEC sensors were of a square geometry 7x7 inches, 8x8 inches, and 9x9 inches and made of 1.25 mil thick copper tape. The sensors conductive trace width was 93.75 mils and the gap width was 31.25 mils. The surface of the panel was coated with dielectric (aerospace) paint and primer, approximately 6mils thick.

Fig. 1. Actual Test Panel with 7 inch SansEC (shown unpainted)

MODELING TOOL

Modeling and simulation of electromagnetic phenomena is an indispensable design tool at any stage and for any scale of an electrical engineering research problem. The FEKO computational electromagnetic software tool was used to develop these simulations. FEKO develops computational solutions based on the integral formulation of Maxwell's equations and uses the Method of Moments (MoM) among other types of solvers. [5]

In the FEKO software package, all geometries were created and designed in CAD FEKO. The physical geometry of the test panels were accurately represented in the FEKO model. Variables defined in CAD FEKO were used to assign material properties and geometry. The simulated panels, as shown in Figure 2, were constructed with 0.15 inch thick FRP defined by a relative permittivity ε_r of 4, a loss tangent $Tan\delta$ of 0.017, and a mass density of 1850 kg/m^3. Although the FRP of the panel was 0.25 inches, the FRP of the panel was simulated at 0.15 inches to simplify computation. The conductive ground paths that encompassed the edges of the panel of the 7 inch, 8 inch and 9 inch SansEC sensors were accurately modeled in the geometry. The dielectric paint over the test panel was modeled with a ε_r of 2.5 and mass density of 1198.26 kg/m^3. The computational model did not include a primer layer under the paint, which was used in the experimental model. [6]
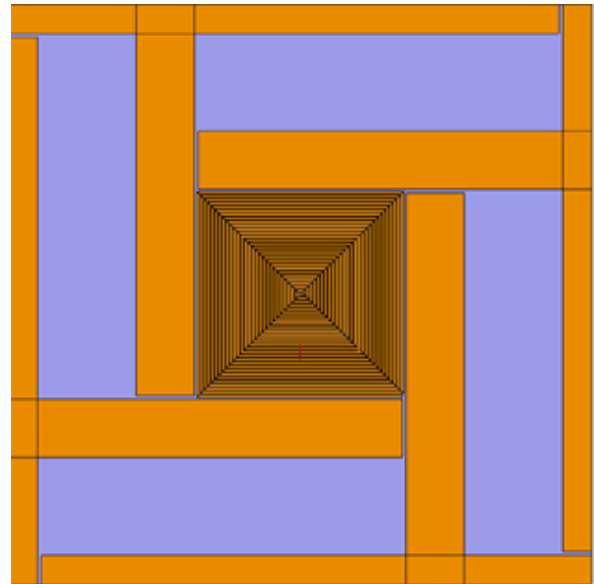

Fig. 2. FEKO Model of Test Panel Geometry (shown unpainted)

Once the physical characteristics were developed in the most plausible detail and design, the digital representation of the panels were simulated using electromagnetic numerical methods in the frequency domain. An electromagnetic field was incident upon the test panel in FEKO using a near field loop antenna. An electromagnetic field is hypothesized to precede an actual lightning strike leader. The simulations calculated the Electric and Magnetic fields at a very close distance to the SansEC geometry. The E-field distributions represent the electric field in the near field of the SansEC conductive trace for a given frequency and likewise with the H-field distributions that represent the magnetic field. [7][8][9]

The simulations ran on a 64-bit operating system computer with an Intel Xeon CPU E5-1650 that ran at a clock speed of 3.20 Gigahertz and had 32 Gigabytes of installed random access memory. The simulation total run time for the 7 inch was 3 hours: 59 minutes: 5seconds and it used approximately 242.744 megabytes of memory per process. The total run time for the 8 inch simulation was 7 hours: 47 minutes: 19 seconds and it used approximately 295.194 megabytes of memory per process. The total run time for the 9 inch was 19 hours: 1 minute: 35 seconds and it used approximately 976.457 megabytes of memory per process. For each simulation, 100 points were requested to sufficiently identify the E-field and H-field structure of the SansEC sensors in the study presented in this paper.

SIMULATION RESULTS

7 Inch SansEC

The 7 inch SansEC sensor reflection coefficient frequency plot in decibel magnitude is shown in Figure 3. The primary resonance frequency is at approximately 57 MHz at a level of -26 dB. The second largest resonance occurs just below 48 MHz at -14 dB. These are fairly strong resonances and are more than adequate to perform sensing in a FRP. Strong resonance phenomena is diminished above 100 MHz.
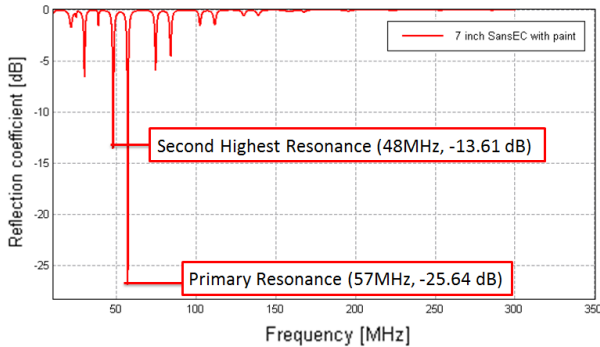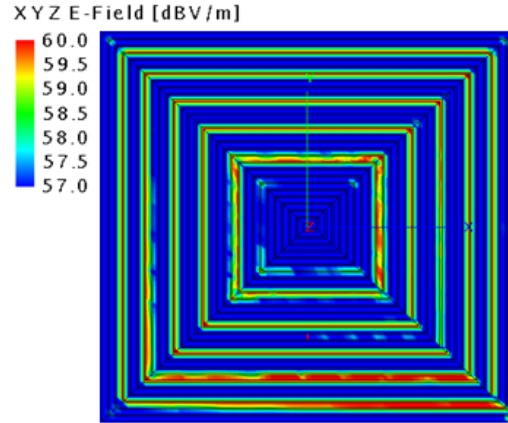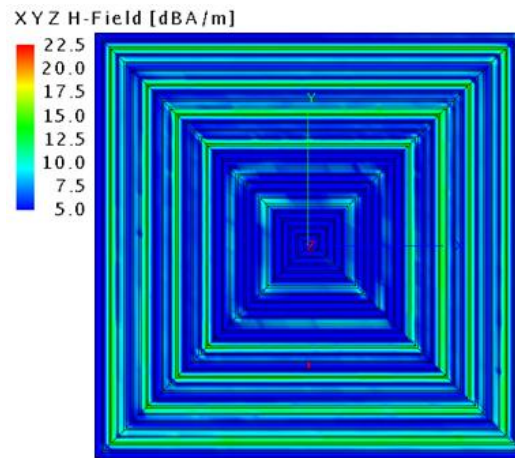

Fig. 3. Reflection Coefficient of the 7 inch SansEC sensor

Figure 4 presents the electric and magnetic field distribution in dBV/m and dBA/m respectively for the 7 inch SansEC sensor. The simulation contained the full panel with grounds, but only the SansEC sensor fields are presented. The amplitude scales were selected to provide visual contrast between high field regions and low field regions. Figure 4.i clearly shows five distinctive loops of high electric field at the primary resonance frequency. Figure 4.ii shows four distinct loops of high magnetic field also at the same frequency. Note both images have no significant field strength at the center of the spiral and at the outer end of the spiral. The open circuit nature of the SansEC sensor requires no current flow at the ends of the trace and thus the field strength diminishes to zero.

(i) E-field of 7 inch SansEC sensor at 57 MHz

(ii) H-field of 7 inch SansEC sensor at 57 MHz

Fig. 4. E-field and H-field of 7 inch SansEC sensor at primary resonance

8 Inch SansEC

The 8 inch SansEC reflection coefficient frequency plot is shown in Figure 5. The primary resonance of the 8 inch SansEC sensor is -21 dB at approximately 51 MHz. The second highest resonance is about -14 dB at approximately 58 MHz. Strong resonance phenomena is diminished above 100 MHz.

Figure 6 presents the electric and magnetic field distribution for the 8 inch SansEC sensor at 51 MHz in the same format as presented for the 7 inch. The E-field distribution shows six loops with higher field while the H-field distribution shows five.
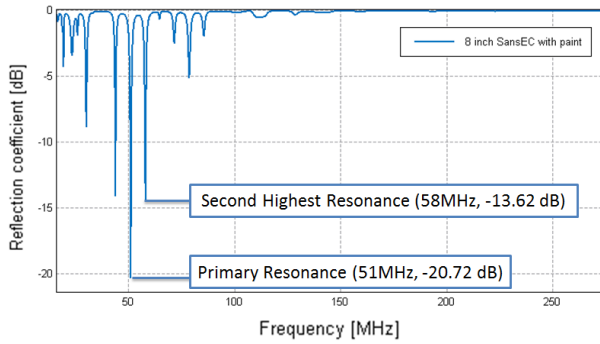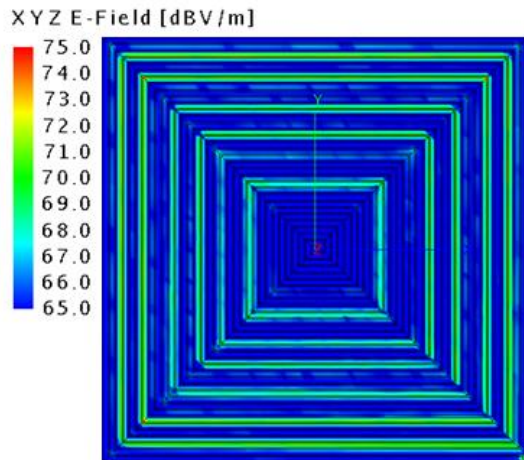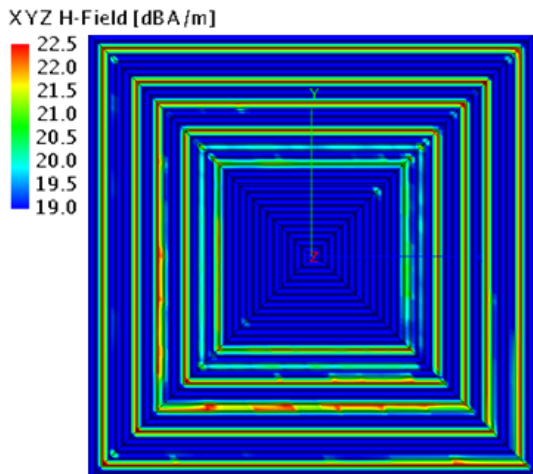
Fig. 5. Reflection Coefficient of the 8 inch SansEC sensor

(i) E-field of 8 inch SansEC sensor at 51 MHz

(ii) H-field of 8 inch SansEC sensor at 51 MHz

Fig. 6. E-field and H-field of 8 inch SansEC sensor at fundamental resonance

9 Inch SansEC

The 9 inch SansEC reflection coefficient frequency plot is shown in Figure 7. The primary resonance of the 9 inch SansEC sensor is -34 dB at approximately 52 MHz. The second highest resonance is around -15 dB at approximately 58 MHz. Again strong resonance phenomena is observed to be diminished above 100 MHz.

Figure 8 presents the electric and magnetic field distribution for the 9 inch SansEC sensor at 52 MHz in the same format as presented earlier. The E-field distribution again shows six distinctive loops with higher electric field. The H-field distribution does not show the distinctive loops of relatively higher magnetic field regions as was observed in the 7 inch and 8 inch sensors. Instead, it appears that nearly all of the traces of the 9 inch sensor generate magnetic field activity at the resonance frequency. The center of the spiral and outer edge are still shown to have minimal magnetic field.
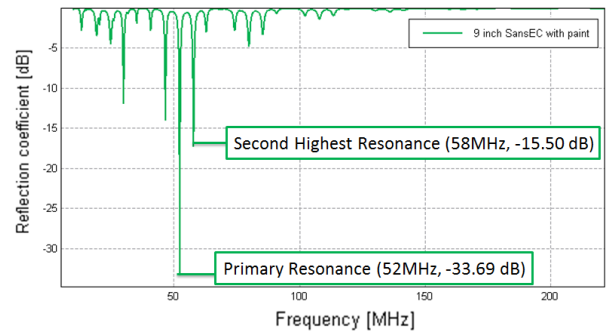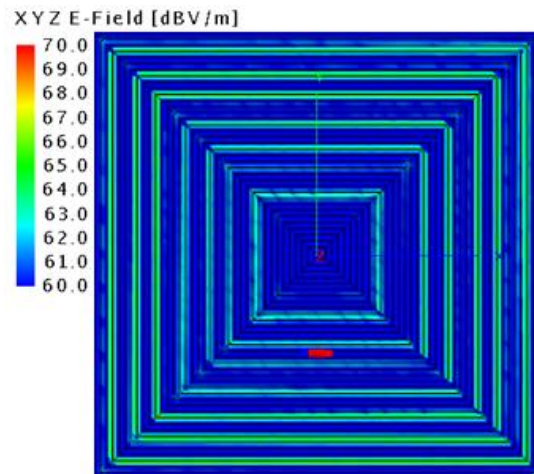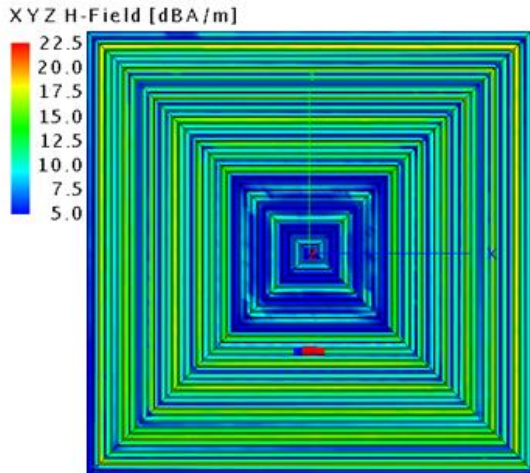

Fig. 7. Reflection Coefficient of the 9 inch SansEC sensor

(i) E-field of 9 inch SansEC sensor at 52 MHz

61.5

(ii) H-field of 9 inch SansEC sensor at 52 MHz

Fig. 8. E-field and H-field of 9 inch SansEC sensor at fundamental resonance

DESCRIPTION OF EXPERIMENT

Lightning tests were conducted at the National Technical Systems' (NTS) Lightning Technologies (LTI) facility in Pittsfield, MA in February, 2012. The SansEC lightning strike protection (LSP) configurations were bonded on fiberglass panels and tested with components D, B & C with a peak current of 40KA. [10]

The SansEC LSP test articles were mounted in a lightning test bed during strike to monitor the electric current on the four sides of the test panel to determine the propagation direction of the electric current. Four Pearson 4418 Current Probes were used to monitor the electric ground current off the edges of the FRP panel. The lightning electrode was positioned at the center of the SansEC sensor for each test. Figure 9 shows a photograph of a carbon fiber test panel installed in the test bed. Pearson probe current monitors are visible in the photo at the corners of the test panel.

The test bed was also instrumented with an IR camera to measure the backside temperatures during the lightning strike. The IR images will show higher temperatures at the lightning attachment locations and along the current pathways from resistive heating. Figure 10 shows a photograph of the IR camera positioned on the back side of the test panel.
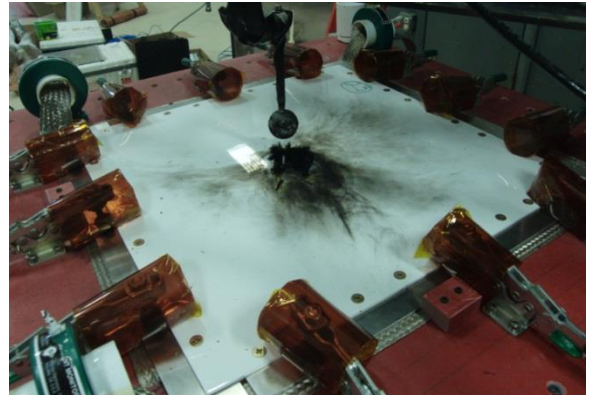

Fig. 9. Photograph of carbon fiber test panel installed in test bed at LTI.

Fig. 10. Photograph of IR Camera used in test bed to capture backside temperatures at LTI.

EXPERIMENTAL RESULTS

7 Inch SansEC

The electric currents measured for the 7 inch SansEC LSP configuration are shown in Figure 11. All the electrical current is shown to travel in channel 2 and 3. The second amplitude peak visible in the unipolar waveform at .1 ms is an artifact of a resistor flashover short in the resistor bank of the lightning current generating system during the strike.

Figure 12 shows a photograph of the post strike panel with graphical representation of the ground paths to identify the current channels. Channel 2 is attached to the left edge of the panel and is attached to the ground path beneath the SansEC in the photo. Channel 3 is on the bottom edge and is attached to the ground path on the right side of SansEC in the photo. Electric current exiting the

bottom right corner of the SansEC could become attached to ground by either channel 2 or 3. The action integral was calculated for each channel to determine the ratio of energy along each path. Channel 2 shows 80% of the total energy and channel 3 has 20%.
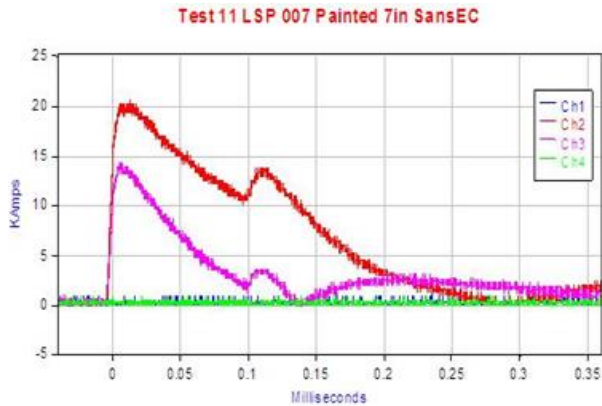

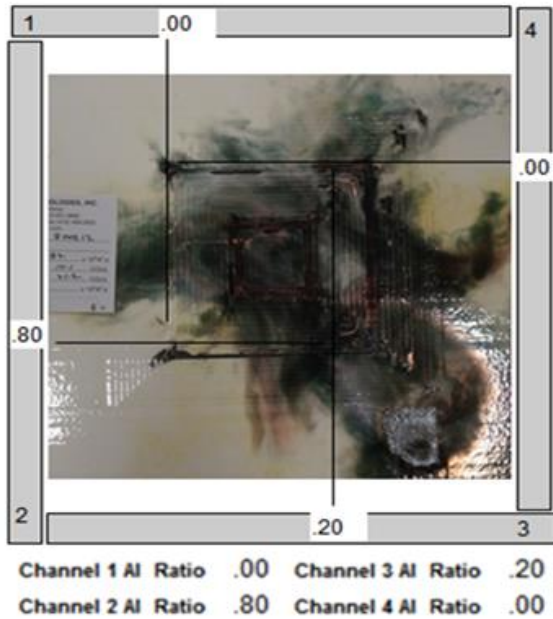Fig. 11. Measured Electric Currents on 7 inch SansEC sensor

Channel 1 Al Ratio .00   Channel 3 Al Ratio .20
Channel 2 Al Ratio .80   Channel 4 Al Ratio .00

Fig. 12. Post Lightning Strike Damage to 7 inch SansEC sensor

A thermal image of the 7 inch SansEC LSP configuration is shown in Figure 13. The IR images are inverted to represent a front side depiction since the thermal data was collected from the back side of the strike. The hotter temperatures represent the location of lightning attachment or current propagation. If a portion of the SansEC trace is immediately destroyed/removed off the panel the IR image may not sense an increase in temperature at that location. Figure 13 shows higher temperatures at the intersection of the ground paths attached to channel 2 and 3 at the lower right corner of the SansEC sensor. Even though the sensor is electrically conductive everywhere, the resistive heating did not occur uniformly over the sensor traces. Note the absence of resistive heating in the center of the sensor. On the right side of the sensor, five separate traces appear to have higher temperature.
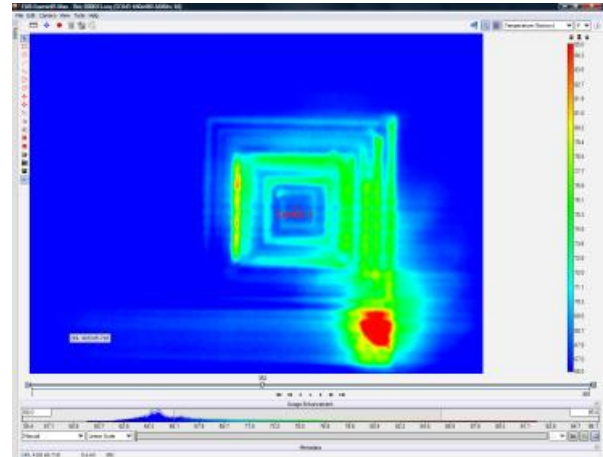

Fig. 13. Infra red Thermal image on 7 inch SansEC sensor

8 Inch SansEC

The current plot for the 8 inch SansEC LSP configuration is shown in Figure 14. All the lightning current was measured in channel 2. The second amplitude peak was again caused by a resistor flashover short.
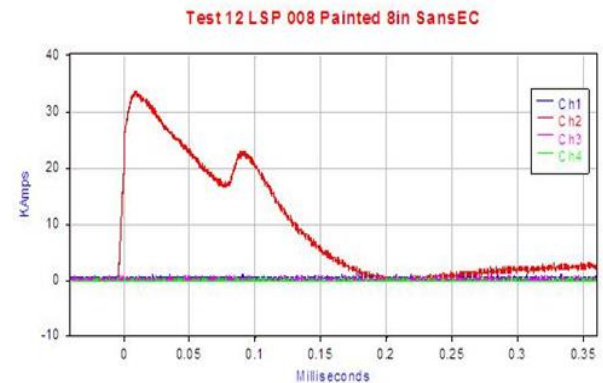

Fig. 14. Measured Electric Currents on 8 inch SansEC sensor

A photograph of the post strike panel and graphical representation of the ground paths with action integral percentages are shown in Figure 15. Burnt traces on the sensor and ground paths can be seen in the photograph. The IR image for this test configuration is shown in Figure 16. The ground path for channel 2 has the highest temperature values. The image is similar in nature to the 7 inch IR image but with six traces on the right side showing higher temperatures.
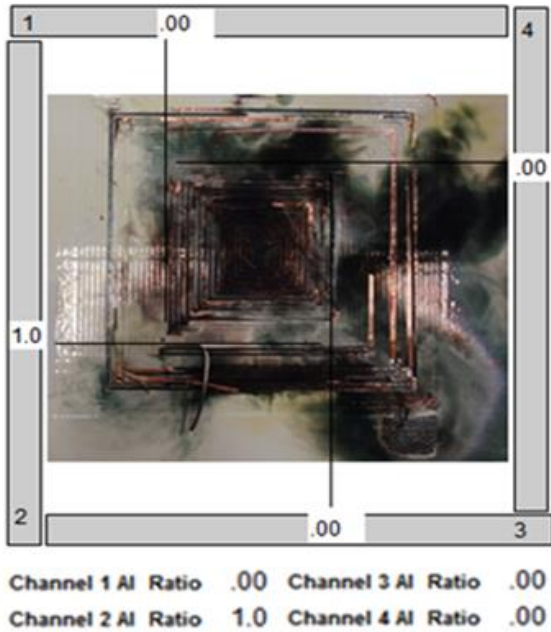

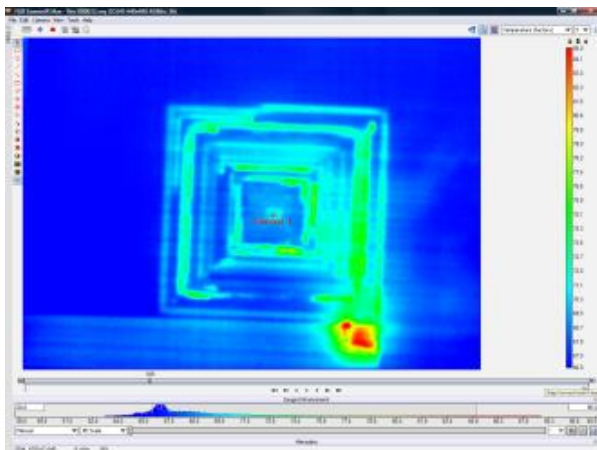Fig. 15. Post Lightning Strike Damage to 8 inch SansEC sensor

Fig. 16. Infra red Thermal image on 8 inch SansEC sensor

9 Inch SansEC

The current plot for the 9 inch SansEC LSP configuration is shown in Figure 17. All the lightning current once again was measured in one channel, but in this case channel 3. The same second amplitude peak around 1 ms is visible in the data from the resistor flashover short.
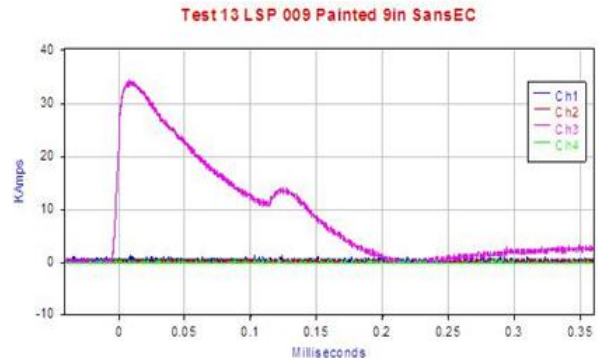

Fig. 17. Measured Electric Currents on 9 inch SansEC sensor

A photograph of the 9 inch LSP configuration post strike panel and graphical representation of the ground paths with action integral percentages are shown in Figure 18. The photo shows burn marks at the upper right corner of the 9 inch SansEC. The IR image for this test configuration is shown in Figure 19. The ground path for channel 3 has the highest temperature values. The image shows much more heating across the top portion of the SansEC traces than in the other two configurations.
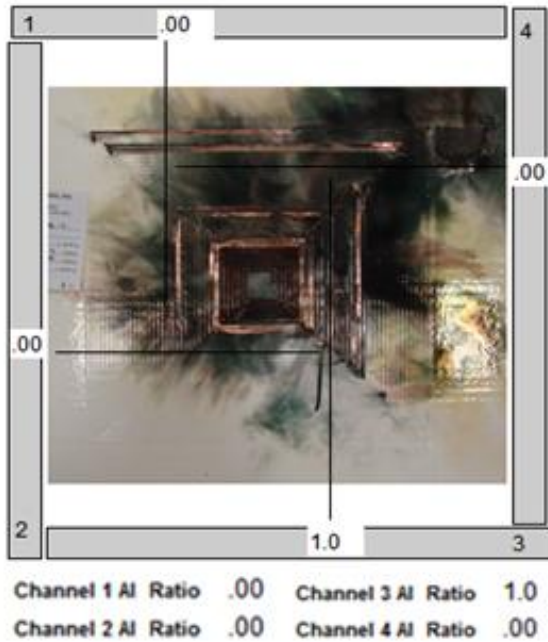
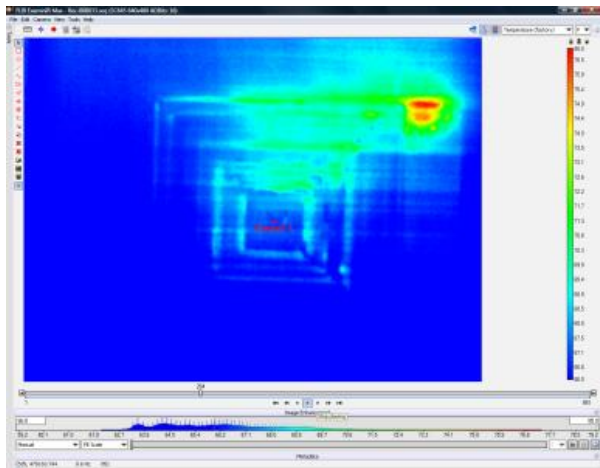Fig. 18. Post Lightning Strike Damage to 9 inch SansEC sensor

Fig. 19. Infra red Thermal image on 9 inch SansEC senor

DATA COMPARISON

7 Inch SansEC

The E-field distribution of the 7 inch SansEC conductive trace at the primary resonance is shown appropriately sized next to the 7 inch lightning test IR image in Figure 20. A slice of the IR image from above the center line has been pasted over the E-field distribution to help visually align the location of the hotter traces next to the higher E-field traces. The five high electric field traces on the right side of the E-field distribution seem to align well with the five higher temperature traces in the right side of the IR image. The area of lower electric field in the center of the E-field distribution appears to coincide with the area of lower temperature in the IR image. High E-field regions occurring at other resonance frequencies are not studied here, but could also play a role in lightning attachment to the sensor.
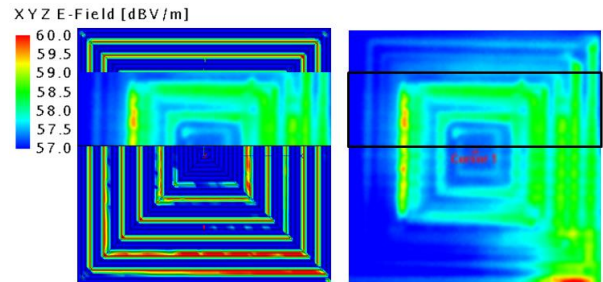

Fig. 20. 7 inch SansEC E-field at 57 MHz (primary resonance) compared with IR image

8 Inch SansEC

The E-field distribution of the 8 inch SansEC conductive trace at the primary resonance is shown appropriately sized next to the 8 inch lightning test IR image in Figure 21. A slice of the IR image from above the center line has been pasted over the E-field distribution to help visually align the location of the hotter traces next to the higher E-field traces. The six high electric field traces on the right side of the E-field distribution seem to approximate the location of the six higher temperature traces in the right side of the IR image. The area of lower electric field in the center of the E-field distribution is reasonably close to the area of lower temperature in the IR image.
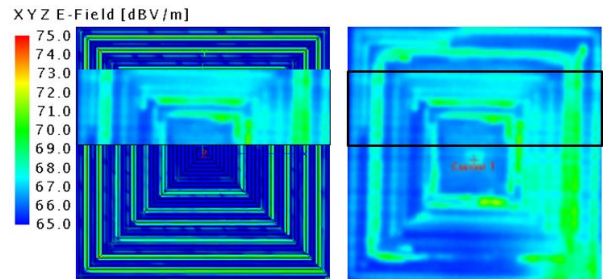

Fig. 21. 8 inch SansEC E-field at 51 MHz (primary resonance) compared with Infra red Thermal image

9 Inch SansEC

The E-field distribution of the 9 inch SansEC conductive trace at the primary resonance is shown appropriately sized next to the 9 inch lightning test IR image in Figure 22. A portion of the IR image from upper left corner has been pasted over the E-field distribution to help visually align the location of the hotter traces in this area next to the higher E-field traces. The traces above center line appear to align reasonable well and are in good agreement at the upper left loop corners. The area of lower electric field in the center of the E-field distribution is reasonably similar to the area of lower temperature in the IR image.
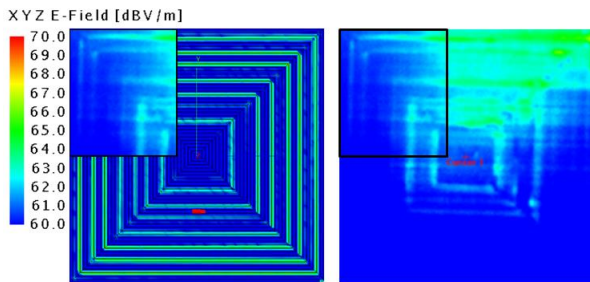

Fig. 22. 9 inch SansEC E-field at 52 MHz (primary resonance) compared with IR image

The data represented in Figure 22 is repeated and shown in Figure 23 with a different dBV/m scale to further show correlation. The E-field scale has been compressed to highlight the higher field regions appearing at the upper right corner. A slice of the E-field distribution from the upper right corner is shown overlaid on the IR image. The E-field distribution shows very high relative field values at this corner and corresponds to the higher temperatures shown in the IR image.
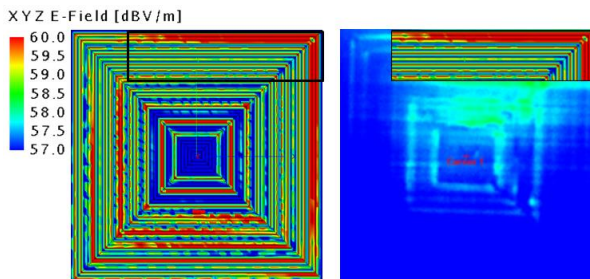

Fig. 23. 9 inch SansEC E-field at 52 MHz (primary resonance) at different dBV/m scale compared with IR image

CONCLUSION

NASA Langley Research Center (LaRC) has conducted research to develop an open circuit SansEC (Sans Electric Connection) sensor to provide lightning strike protection (LSP) in conjunction with damage detection and diagnosis. [1] [2]

Lightning-direct effect current tests were conducted on multiple SansEC sensor configurations on FRP substrates. Test results have shown the 7 inch, 8 inch, and 9 inch square SansEC configurations have an intrinsic ability to guide the lightning energy in one direction based on test results from current measurements made on the four sides of the test panels and back side IR imagery. IR temperature measurements provide a visual means to show electrical resistive heating from lightning attachment and current propagation on the SansEC geometry.

Electromagnetic computational simulations were conducted using FEKO to determine the sensor's primary resonance frequency and electric field distribution just above the surface of the SansEC sensor's conductive trace at its primary resonance. The SansEC sensors presented here resonate at frequencies within the lightning radiated spectrum.

The E-field distribution was compared to the lightning test IR image to correlate the locations of high E-fields to the higher temperatures seen in the IR image. All three sensors showed reasonable correlation between the high E-field regions to the locations with higher temperature and lightning attachment or current propagation. It is noted that traces that have been immediately burned away or destroyed would not show increased temperatures in the IR image. These correlation results suggest the higher electric field regions on the SansEC sensor at resonance influence the attachment and propagation of the lightning energy. The study suggests the lightning attachment on the SansEC sensor occurs at the higher electric field regions resident on the conductive trace at its primary resonance frequency. Higher relative E-fields at other resonance frequencies may also influence attachment but were not included in this study.

REFERENCES

[1] C. Wang, K. Dudley, G. Szatkowski, "Open Circuit Resonant (SansEC) Sensor for Composite Damage Detection and Diagnosis in Aircraft Lightning Environments," American Institute of Aeronautics and Astronautics, 8, June 25, 2012

[2] S. Woodard, "SansEC Sensing Technology - A New Tool for Designing Space Systems and Components", Aerospace Conference, 2011.

[3] Franklin A. Fisher, J. Anderson Plumer, "Lightning Protection of Aircraft", Volume 1008 of NASA reference publication, United States National Aeronautics and Space Administration (NASA), 1977-2004

[4] D. M. Le Vine, " Review of measurements of the RF spectrum of radiation from lightning", Meteorology and Atmospheric Physics, Volume 37, Issue 3, pp 195-204, 1987

[5] EMSS, "FEKO Comprehensive Electromagnetic Solutions User's Manual", EM Software & Systems-S.A. (Pty) Ltd. 32 Techno Avenue, Technopark, Stellenbosch, 7600, South Africa, 2011

[6] U. Jakobus, J.J. Van Tonder, "Fast Multipole Solution of Metallic and Dielectric Scattering Problems in FEKO", 21st Annual Review of Progress in Applied Computational Electromagnetics, Applied Computational Electromagnetics Society (ACES) 2005

[7] L.J. Smith, K.L. Dudley, G.N. Szatkowski, "Computational Electromagnetic Modeling of SansEC Sensors", 27th International Review of Progress in Applied Computational Electromagnetics; (ACES) Williamsburg, VA; 27-31 Mar. 2011

[8] V.A. Rakov, "Characterization of Lightning Electromagnetic Fields and Their Modeling", University of Florida, Gainesville, USA

[9] D.E. Crawford, V. A. Rakov, M. A. Uman, G. H. Schnetzer, K. J. Rambo, M. V. Stapleton, and R. J. Fisher, "The close lightning electromagnetic environment: Dart-leader electric field change versus distance", J. Geophys. Res., 106(D14), 14909–14917, 2001

[10] Ed Rupke, "Lightning Direct Effects Handbook", Lightning Technologies Inc. 10 Downing Industrial Parkway, Pittsfield, MA, March 1, 2002